severe obesity. Basically, CRP mRNA levels are correlated positively with those of IL-6 and the liver, and also adipose tissue, and can produce CRP, a process which could be dependent on IL-6.[8] These findings suggest a role for IL-6 as a proinflammatory cytokine in the development of NASH. Moreover, latest reports have shown that hepatocyte IL-6 expression correlated positively with plasma IL-6 levels and the degree of hepatic inflammation, stage of fibrosis and systemic insulin resistance.[3,4,9]

From a different point of view, IL-6 is well known to be a hepato-protective cytokine. IL-6 acts directly on hepatocytes, inducing the translocation of signal transducer and activator of transcription (STAT)3 to the nucleus causing early gene activation and mitosis.[10,11] The IL-6/soluble IL-6 receptor fusion protein led to an earlier onset of hepatocellular proliferation and had an important role in liver regeneration after partial hepatectomy in mice.[12] This signaling not only has an effect on hepatocyte proliferation but also protects the liver against various forms of injury, such as ischemia and reperfusion, toxins, alcohol and death-mediated Fas activation.[13–15] Mice lacking IL-6 have an impaired ability to regenerate their livers after partial hepatectomy, increased caspase 3/8 activities and reduced antiapoptotic mediators.[6,14,16,17] Short-term replacement of IL-6 also might protect the liver through preservation and restoration of intrahepatic adenosine triphosphate (ATP) levels, which have been reported to be reduced in fatty livers.[18]

Chronic inflammation is a risk for the development of fibrosis and carcinogenesis in various organs.[19,20] Controlling the inflammation would prevent the progression of this process, even if it may not be able to stop the occurrence of the diseases altogether. Recently, inhibition of the proinflammatory cytokine signaling pathway using neutralizing antibody against the IL-6 receptor (tocilizumab, which is a specific antagonist of the human IL-6 receptor and soluble IL-6 receptor) has been reported to improve chronic inflammatory diseases, such as rheumatoid arthritis, in clinical practice.[21] In this study, to evaluate the possible role of IL-6 in the development of hepatic steatosis and NASH, we tested a rat anti-mouse IL-6 receptor antibody, MR16-1, a specific antagonist of the mouse IL-6 receptor, in mouse NASH models. Feeding mice with an MCD diet induces steatohepatitis and liver fibrosis, providing a useful small animal model for NASH.[22] Using this model, we found that, although treatment with MR16-1 enhanced hepatic steatosis, it ameliorated liver injury. Neutralizing the IL-6 receptor by MR16-1 for 8 weeks suppressed IL-6/Glycoprotein130 (GP130) signaling successfully and decreased expression of suppressor of cytokine signaling (SOCS)3 in correlation with decreased plasma free fatty acid (FFA) levels, hepatic Cyp2E1 expression, evidence of lipid peroxidation/oxidant stress and hepatocyte apoptosis. In conclusion, inhibiting IL-6/GP130 signaling enhanced hepatic steatosis, but ameliorated liver damage in mice with MCD diet-induced NASH.

MATERIALS AND METHODS

Animals and Treatments

A mouse model of MCD diet-induced NASH was studied. Six-week-old male C57/BL6 mice were purchased from Japan Jackson Laboratories, maintained in a temperature- and light-controlled facility and permitted consumption of water *ad libitum*. In all, 5 mice were fed a control chow diet (cat no. 960441; ICN, Aurora, OH) and 10 were fed an MCD diet (cat no. 960439; ICN) for 8 weeks. Half of the MCD diet-fed mice ($N=5$) were treated with 15 mg/kg rat anti-mouse IL-6 receptor antibody (MR16-1; Cyugai Pharmaceutical, Tokyo, Japan) intraperitoneally twice weekly, the remainder ($N=5$) and five chow-fed mice were injected with control rat IgG (Equitech-Bio, Kerrville, TX).[23,24] All animal experiments fulfilled the requirements for humane animal care in the Kyoto Prefectural University of Medicine.

Immunoblot Assay

Nuclear proteins isolated using a NE-PER Nuclear Extraction Reagent Kit (Pierce Biotechnology, Rockford, IL) and proteins isolated from whole livers were electrophoresed in SDS-PAGE gels and transferred to PVDF membranes. The membranes were probed with anti-sterol regulatory element-binding protein (SREBP)-1 (Santa Cruz Biotechnology, sc-366 for the precursor and sc-367 for the mature fragment, Santa Cruz, CA), anti-peroxisome proliferator-activated receptor (PPAR)α (LifeSpan Biosciences, WA), anti-4-hydroxy-2-nonenal (HNE) (HNEJ-2; Nikken, Shizuoka, Japan), anti-cytochrome P4502E1 (Cyp2E1) (Stressgen, Victoria, Canada), anti-catalase (Abcam, Cambridge, MA) anti-STAT3, anti-phospho-STAT3, anti-Akt, anti-phospho-Akt (ser473), anti-adenosine monophosphate-activated protein kinase (AMPK), anti-phospho-AMPK (Thr172), (Cell Signaling Technology, Beverly, MA) antibody, anti-α-actin (Santa Cruz Biotechnology) antibody or anti-glyceraldehydes-3-phosphate dehydrogenase (GAPDH) (Santa Cruz Biotechnology) antibody, followed by horseradish peroxidase (HRP)-conjugated anti-mouse or rabbit IgG (Amersham, UK). Antigens were visualized by ECL (Amersham). Immunoblots were scanned, and band intensities were quantified by Image J (NIH) densitometry analysis.

Two-Step Real-Time RT-PCR

Real-time PCR was performed as described previously.[25] Specificity was confirmed for all primer pairs (Table 1) by sequencing the PCR products. Target gene levels are presented as a ratio of levels in treated *vs* corresponding control groups. Fold changes were determined using point and interval estimates.

Immunohistochemistry and Analysis of Liver Architecture

Serial sections were stained with H&E using standard techniques. After deparaffinization, microwave antigen retrieval and blocking endogenous peroxidase activity, other sections were incubated with a TdT-mediated dUTP-digoxigenin

nick-end labeling (TUNEL) reaction mixture, containing terminal deoxyribonucleotidyl transferase (TdT) and fluorescein-dUTP (Roche Diagnostic, Indianapolis, IN), or anti-α-smooth muscle actin (SMA) (DakoCytomation, Carpinteria, CA) antibody. Antigen was demonstrated using secondary anti-mouse polymer HRP and DAB chromagen (DakoCytomation) and counterstaining with Gill's hematoxylin. The number of TUNEL-positive hepatocytes was counted in three randomly selected fields per section (× 100 magnification).

Table 1 RT-PCR primers for analysis

Gene	Direction	Sequence
Gus	Forward	GCAGTTGTGTGGGTGAATGG
	Reverse	GGGTCAGTGTGTTGTTGATGG
SOCS3	Forward	GGGTGGCAAAGAAAAGGAG
	Reverse	GTTGAGCGTCAAGACCCAGT
TNFα	Forward	TCGTAGCAAACCACCAAGTG
	Reverse	AGATAGCAAATCGGCTGACG
TGFβ-1	Forward	TTGCCCTCTACAACCAACACAA
	Reverse	GGCTTGCGACCCACGTAGTA
Pro Colα1	Forward	GACATCCCTGAAGTCAGCTGC
	Reverse	TCCCTTGGGTCCCTCGAC
α-SMA	Forward	AAACAGGAATACGACGAAG
	Reverse	CAGGAATGATTTGGAAAGGA
FATP1	Forward	CGCTTTCTGCGTATCGTCTG
	Reverse	GATGCACGGGATCGTGTCT
FATP2	Forward	GGTATGGGACAGGCCTTGCT
	Reverse	GGGCATTGTGGTATAGATGACATC
FATP5	Forward	CTACGCTGGCTGCATATAGATG
	Reverse	CCACAAAGGTCTCTGGAGGAT

Quantification of Hepatic Collagen Content

Sirius red staining was performed on 4-μm-thick paraffin sections of liver tissues fixed in buffered formalin. After deparaffinization, the sections were treated with 0.1% Sirius Red F3B (Sigma-Aldrich, Japan) and 0.1% Fast Green FCF (Sigma-Aldrich) in saturated Picric acid solution (Sigma-Aldrich) for 30 min. Sirius red staining area was quantitated by Image J software in three randomly selected fields per section (× 200 magnification).

Tissue and Plasma Biochemical Measurements

Plasma alanine aminotransferase (ALT), FFA, total cholesterol, triglyceride and glucose levels were measured as described previously.[25] Plasma IL-6, serum amyloid A (SAA), TNF-α concentrations and tissue triglyceride were measured using an IL-6 Mouse ELISA Kit (R&D Systems, Minneapolis, MN), SAA mouse ELISA kit (Stressgen), TNF-α mouse ELISA Kit (Invitrogen, Japan) and Triglyceride Detection Kit (Sigma-Aldrich) according to the manufacturers' instructions.

Statistical Analysis

Results are expressed as mean ± s.e.m. Significance was established using Student's *t*-test and analysis of variance when appropriate. Differences were considered significant when $P<0.05$.

RESULTS

An MCD Diet Elevated Plasma IL-6 Levels and Activated Hepatic STAT3 Signaling

We measured plasma IL-6 levels by ELISA in MCD diet-fed mice and compared them with those in chow diet-fed mice. As in previous studies,[26,27] an MCD diet increased IL-6 levels dramatically (Figure 1a) and also activated the expression of a key gene in IL-6/GP130 signaling, STAT3 (Figure 1b). Plasma SAA levels were also increased in MCD diet-fed mice

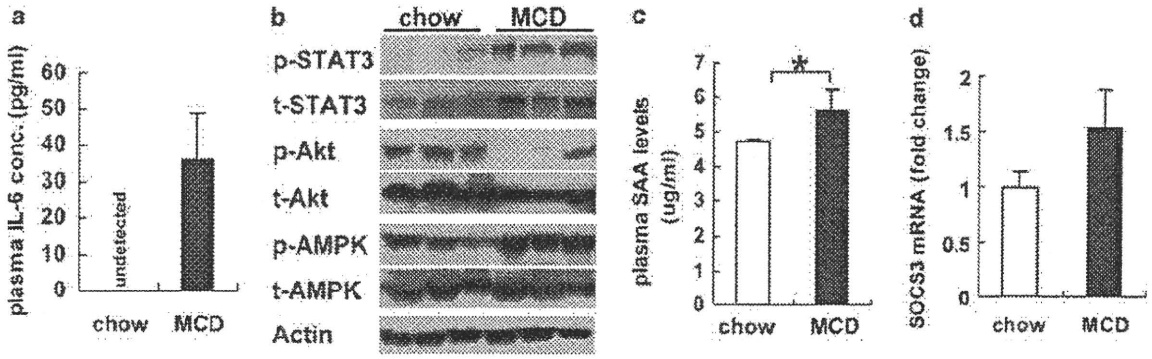

Figure 1 The effect of an MCD diet on plasma IL-6 and SAA levels and hepatic IL-6/ GP130-related gene expression. (**a**) Plasma IL-6 levels were measured. Mean ± s.e. data from each group ($n=5$ per group) are plotted at 8 weeks. (**b**) Phosphorylated (p)-stat3, total (t)-STAT3, p-Akt, t-Akt, p-AMPK and t-AMPK levels were evaluated by immunoblot analysis of livers obtained from three mice per group after 8 weeks. To control for loading, the blot was stripped and reprobed for β-actin, a housekeeping gene. (**c**) Plasma SAA levels were measured. Mean ± s.e. data from each group ($n=5$ per group) are plotted at 8 weeks ($^*P<0.05$). (**d**) mRNA levels of SOCS3 were determined by quantitative real-time PCR analysis of total liver RNA obtained after 8 weeks. Results were normalized to glucuronidase (GUS) expression in each sample and then expressed as fold change relative to gene expression in chow-fed control mice. Mean ± s.e. data from each group ($n=5$ per group) ($P=0.094$).

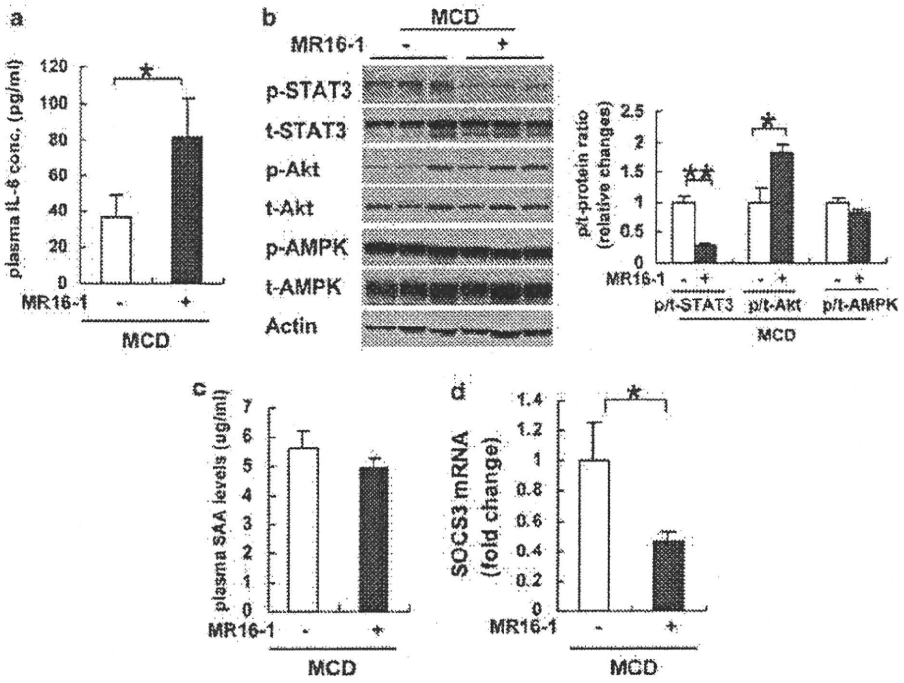

Figure 2 The effect of MR16-1 treatment on plasma IL-6 levels and hepatic IL-6/GP130-related gene expression in MCD diet-fed mice. (**a**) Plasma IL-6 levels were measured. Mean ± s.e. data from each MCD diet-fed group ($n = 5$ per group) are plotted at 8 weeks. (**b**) P-STAT3, STAT3, p-Akt, Akt, p-AMPK and AMPK levels were evaluated by immunoblot analysis of livers obtained from three mice per group after 8 weeks. To control for loading, the blot was stripped and reprobed for β-actin. P-STAT3/t-STAT3, P-Akt/t-Akt and p-AMPK/t-AMPK ratios in each group were also expressed as fold change of control IgG-treated mice (*$P < 0.05$). (**c**) Plasma SAA levels were measured. Mean ± s.e. data from each group ($n = 5$ per group) are plotted at 8 weeks. (**d**) mRNA levels of hepatic SOCS3 were determined by quantitative real-time PCR analysis after 8 weeks of treatment. Results were normalized to GUS expression and then expressed as fold change relative to gene expression in controls. Mean ± s.e. data from each MCD diet-fed group ($n = 5$ per group) (*$P < 0.05$).

(Figure 1c). The expression of genes involved in glucogenesis and lipogenesis, Akt and AMPK, was also assessed. An MCD diet induced AMPK phosphorylation but reduced Akt phosphorylation (Figure 1b). Furthermore, mRNA levels of hepatic SOCS3 were slightly (but not significantly, $P = 0.094$) increased in MCD mice (Figure 1d), suggesting that activation of STAT3 by an MCD diet might inhibit Akt phosphorylation through induction of SOCS3.

Neutralizing the IL-6 Receptor Blocked IL-6/GP130 Signaling

In this study, we used MR16-1 to block the IL-6/GP130 pathway because earlier studies had shown that twice weekly intraperitoneal injections of 15 mg/kg MR16-1 suppressed the IL6/GP130 pathway in mice effectively.[24]

First, to examine the efficacy of MR16-1, we measured plasma IL-6 concentrations after MR16-1 treatment, and found that plasma IL-6 levels were greatly increased. This phenomenon may be caused by decreased clearance of IL-6 from the blood[28] and suggests that MR16-1 treatment blocked the IL-6 receptor successfully (Figure 2a, Supplementary Figure 1A). This treatment had little effect on STAT3 phosphorylation in chow-fed controls but greatly decreased MCD diet-induced STAT3 phosphorylation (Figure 2b, Supplementary Figure 1B). This result showed that profound suppression of hepatic STAT3 activity might be attributed to the inhibition of IL-6 signaling by MR16-1 treatment in MCD diet-fed mice. Moreover, Akt phosphorylation was somewhat recovered by MR16-1 treatment in both chow- and MCD diet-fed mice. In contrast, AMPK phosphorylation seems slightly decreased in MCD diet-fed mice (Figure 2b, Supplementary Figure 1B). MR16-1 treatment had no effect on plasma SAA levels in chow-fed mice, but slightly decreased plasma SAA levels in MCD diet-fed mice (Figure 2c, Supplementary Figure 1C). mRNA levels of hepatic SOCS3 expression were also decreased by >50% in only MCD diet-fed mice (Figure 2d, Supplementary Figure 1D, *$P < 0.05$).

Neutralizing the IL-6 Receptor Exacerbated MCD Diet-Induced Hepatic Steatosis, but it Decreased Plasma FFA Levels

As some reports have shown that the activation of STAT3 improved hepatic steatosis by inhibiting expression of SREBP-1,[11,29] neutralizing the IL-6 receptor might be expected to exacerbate hepatic steatosis. This was evaluated by H&E staining. Steatosis was scored on H&E-stained sections according to Brunt's criteria[30] and photomicrographs from representative mice are shown (Figure 3a, Supplementary Figure 2A). An MCD diet for 8 weeks induced a mild diffuse hepatic steatosis compared with chow diet. Furthermore,

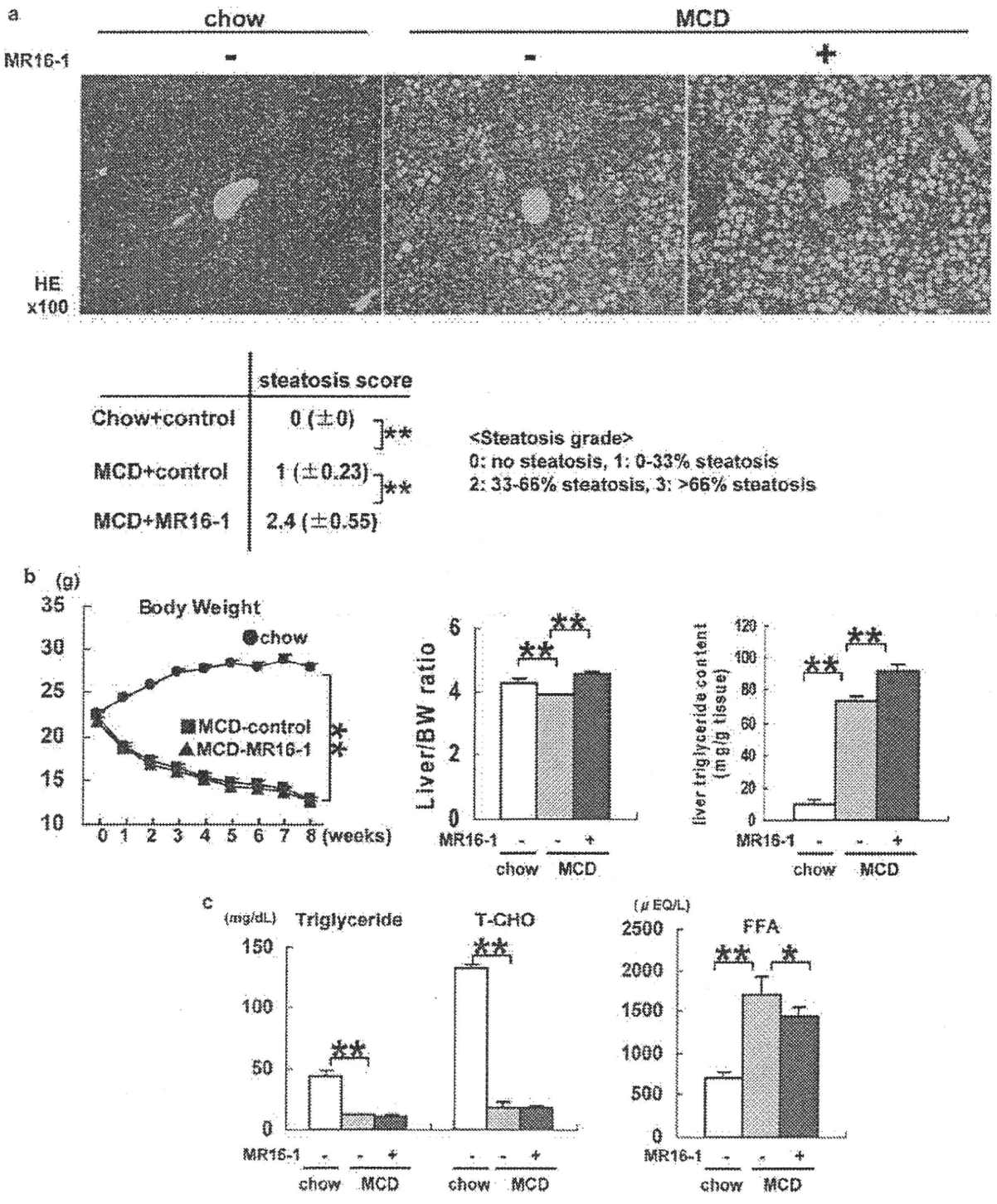

Figure 3 Liver histology, BW, liver/BW ratio, liver triglyceride content and plasma total-cholesterol, triglyceride and FFA levels in chow- or MCD diet-fed mice treated with control IgG or MR16-1. (**a**) Hematoxylin and eosin staining of liver sections from representative mice from each treatment group. Hepatic steatosis grade was assessed on sections obtained from each mouse. Mean ± s.e. data from each group ($n = 5$ per group) are displayed (**$P < 0.01$). (**b**) Body weight (BW) was assessed weekly until the end of the treatment. Liver/BW ratio and liver triglyceride content were determined at the end of the treatment. Results of liver triglycerides are expressed per gram tissue. Mean ± s.e. data from each group are plotted (**$P < 0.01$). (**c**) Plasma total-cholesterol (T-CHO), triglyceride and FFA levels were determined in each group ($n = 5$ per group) at the end of the 8-week treatment period. Data are presented as mean ± s.e. (*$P < 0.05$, **$P < 0.01$).

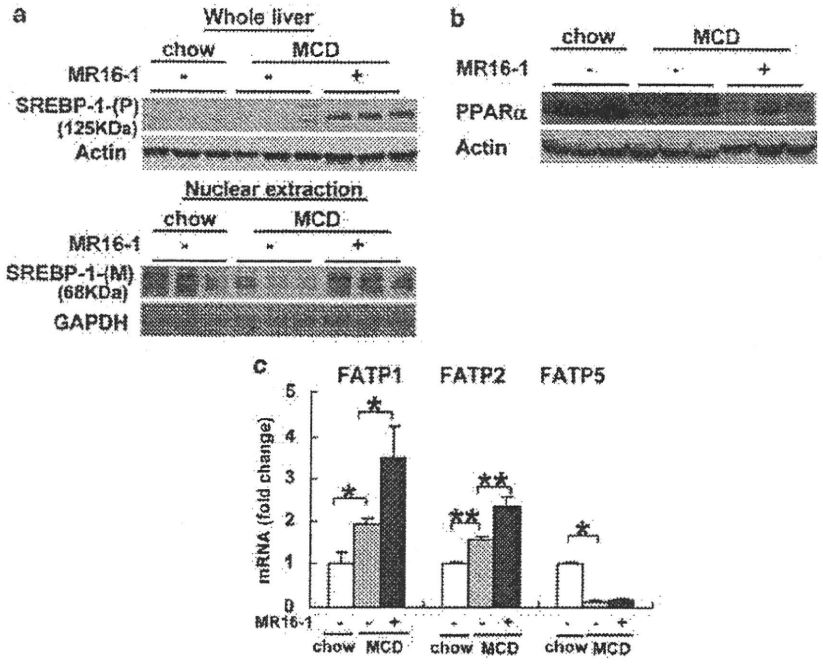

Figure 4 The effect of MR16-1 treatment on hepatic lipogenic and fatty acid uptake-related gene expression. (**a**) SREBP-1 precursor (P) (MW: 125 kDa) and mature soluble fragment (M) (MW: 68 kDa) levels were evaluated by immunoblot analysis of whole livers or nuclear extraction from three mice per group after 8 weeks. To control for loading, the blot was stripped and reprobed for β-actin or GAPDH, respectively. (**b**) PPARα levels were evaluated by immunoblot analysis of livers from three mice per group after 8 weeks of treatment. To control for loading, the blot was stripped and reprobed for β-actin. (**c**) mRNA levels of hepatic FATP1, 2 and 5 were determined by quantitative real-time PCR analysis after 8 weeks of treatment. Results were normalized to GUS expression and then expressed as fold change relative to gene expression in chow-fed control mice. Mean ± s.e. data from each group ($n = 5$ per group) ($^*P < 0.05$, $^{**}P < 0.01$).

MCD diet-fed, but not chow-fed, mice treated with MR16-1 had a greater degree of hepatic steatosis than those treated with control IgG. These findings were confirmed by analysis of body weight (BW), liver/BW ratio and biochemical analysis of hepatic triglyceride content (Figure 3b, Supplementary Figure 2B). Interestingly, MR16-1 treatment attenuated the MCD diet-induced increases in plasma FFA without decreasing plasma triglyceride and total cholesterol levels (Figure 3c, Supplementary Figure 2C).

Neutralizing the IL-6 Receptor Enhanced Hepatic Fatty Acid Synthesis and Uptake

We assessed the protein levels of SREBP-1 expression to investigate their correlation with decreased STAT3 activity and exacerbated hepatic steatosis after MR16-1 treatment. An MCD diet had no effect on the SREBP-1 precursor (molecular weight: 125 kDa) that is attached to the nuclear envelope and endoplasmic reticulum but slightly decreased the mature soluble fragment (molecular weight: 68 kDa) in the nucleus (Figure 4a). MR16-1 treatment increased both forms of SREBP-1 in MCD diet-fed mouse livers (Figure 4a). An MCD diet decreased the protein levels of PPARα, and MR16-1 treatment further accelerated the reduction (Figure 4b). In our study, although the fatty acid transport protein (FATP) 3, 4 (data not shown) and 5 mRNA levels were not altered, FATP 1 and 2 were significantly upregulated in MCD diet-fed mice (but not significantly in chow-fed mice) by MR16-1 treatment (Figure 4c, $^*P < 0.05$, Supplementary Figure 3C).

Neutralizing the IL-6 Receptor had no Effect on MCD Diet-Induced Liver Fibrosis

Hepatic steatosis has been identified as a risk factor for liver fibrosis. Therefore, we assessed liver fibrosis by real-time PCR of mRNA levels of various markers of fibrosis. Although an MCD diet significantly increased mRNA levels of hepatic collagen and transforming growth factor β1 expression, compared with chow control, MR16-1 treatment had no effect on those levels (Figure 5a, $^*P < 0.05$). Sirius red staining and α-SMA immunohistochemistry were performed to further assess the effects of MCD diet and MR16-1 treatment on liver fibrosis. However, MR16-1 treatment had no effect on the area of Sirius red-stained fibrils and α-SMA staining cells (Figure 5b).

Neutralizing the IL-6 Receptor Ameliorated MCD Diet-Induced Liver Injury

To evaluate liver injury after MR16-1 treatment, we compared injury-related parameters. As expected, MCD diet-fed mice exhibited 10-fold higher plasma ALT values than did the controls (Figure 6a). However, plasma ALT values were

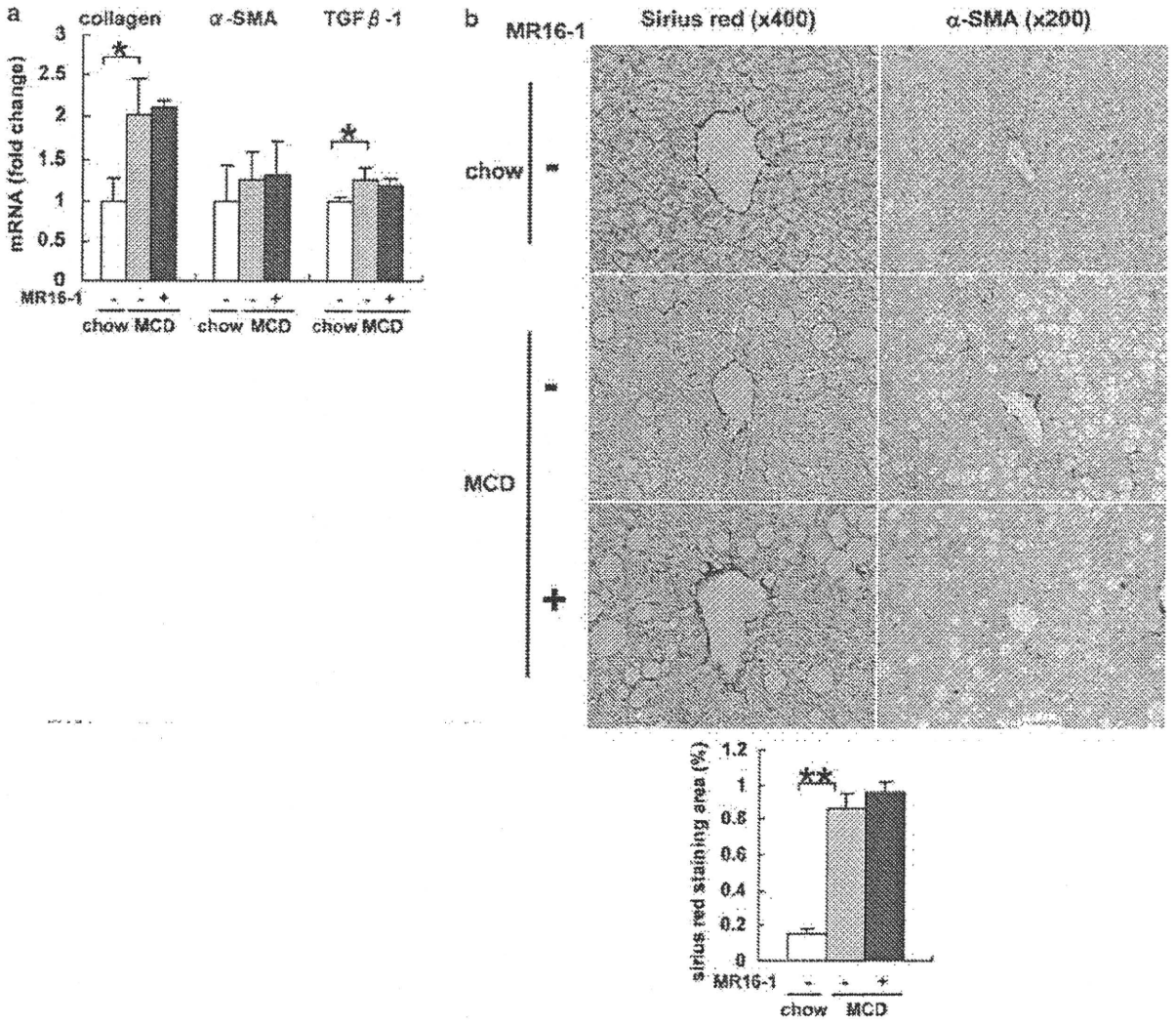

Figure 5 Markers of fibrosis in chow- or MCD diet-fed mice treated by control IgG or MR16-1. (**a**) mRNA levels of hepatic collagen, α-SMA and TGFβ-1 were determined by quantitative real-time PCR analysis after 8 weeks of treatment. Results were normalized to GUS expression. Mean ± s.e. data from each sample are displayed as fold change relative to chow-fed control mice (*$P<0.05$). (**b**) Liver sections from all mice were stained with Sirius red and α-SMA antibody after 8 weeks of treatment. Photomicrographs from representative sections are shown. Morphometric analysis of Sirius red-stained sections from each MCD diet-fed group ($n=5$ per group) at 8 weeks. Results are expressed as % of section staining (+) for Sirius red.

significantly lower in MR16-1-treated mice than in control IgG treated-mice (Figure 6a, **$P<0.01$). These observations were seen only in MCD diet-fed mice (Supplementary Figure 3A). In many mouse models of fatty liver diseases and insulin resistance, as well as in humans with similar conditions, TNF-α has been implicated to have an important role in the pathogenesis of NASH. In this study, however, MR16-1 treatment had little effect on MCD diet-induced elevated plasma TNF-α levels and hepatic TNF-α mRNA expression (Figure 6b, Supplementary Figure 3B). Liver sections were also evaluated for lobular inflammation. The lobular inflammatory grade was higher in MCD diet-fed mice than in chow-fed controls. MR16-1 treatment slightly ameliorated liver injury in MCD diet-fed mice (Figure 6c). To determine why neutralizing the IL-6 receptor in MCD diet-fed mice ameliorated liver injury but exacerbated liver steatosis, we compared the expression of microsomal and peroxisomal FFA-oxidizing enzymes and markers of lipotoxicity. MR16-1 treatment decreased protein levels of hepatic Cyp2E1, catalase and MCD diet-induced 4-HNE expression (Figure 6d). Furthermore, TUNEL staining also showed that MCD diet-induced hepatic apoptosis was decreased by MR16-1 treatment (Figure 6e).

DISCUSSION

According to the 'two-hit' hypothesis, oxidative stress, lymphocyte activation and cytokine release are candidate elements of the pathogenic transition from simple steatosis to

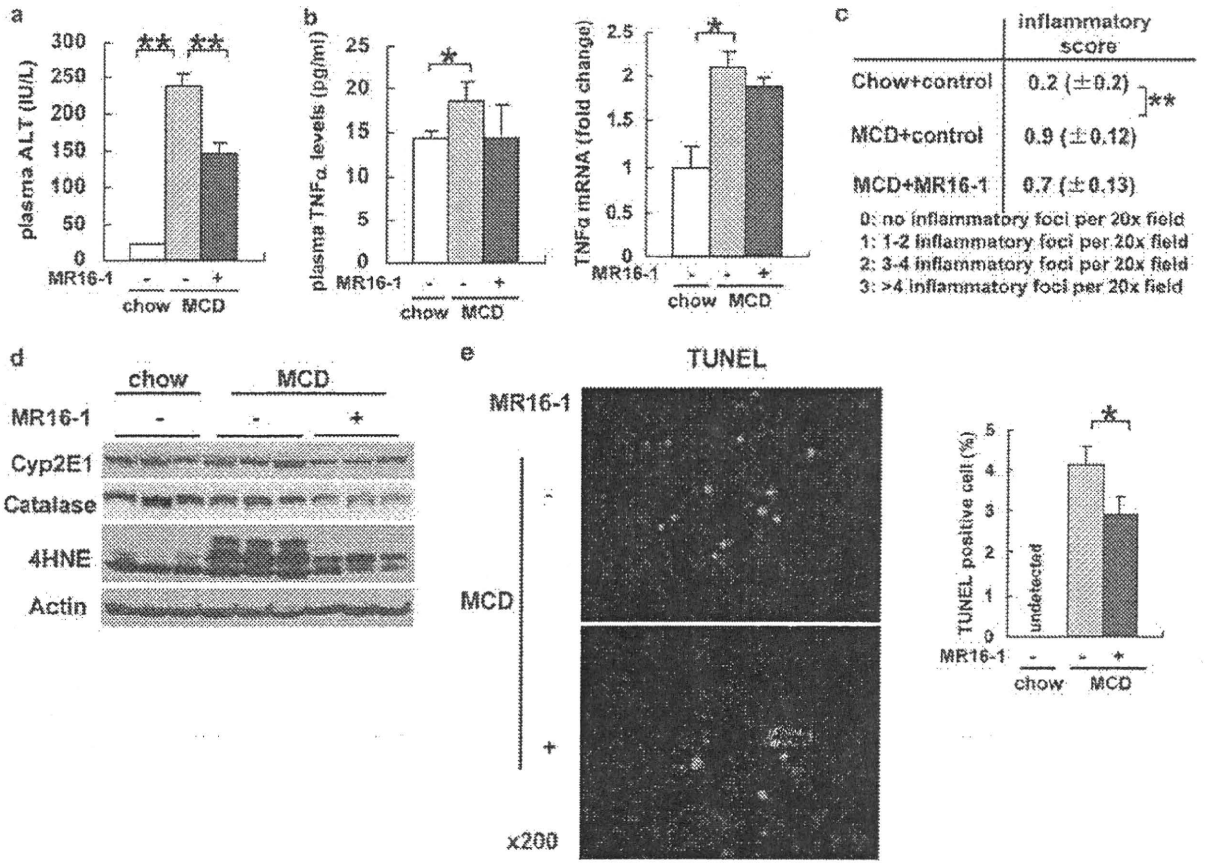

Figure 6 Injury-, lipotoxicity- and apoptosis-related parameters in chow- or MCD diet-fed mice treated by control IgG or MR16-1. (**a**) Plasma ALT levels were measured after 8 weeks of treatment. Mean ± s.e. results from each group ($n = 5$ per group) (**$P < 0.01$). (**b**) Plasma TNF-α levels were measured from each group ($n = 5$ per group) at 8 weeks. The mRNA levels of hepatic TNF-α were also evaluated by quantitative real-time PCR analysis. Results were normalized to GUS expression. Mean ± s.e. data are relative to chow-fed control mice (*$P < 0.05$). (**c**) The number of inflammatory foci per × 20 field was counted on sections obtained from each mouse. Mean ± s.e. data from each group ($n = 5$ per group) are displayed (**$P < 0.01$). (**d**) Cyp2E1, catalase and 4-HNE levels were evaluated by immunoblot analysis of livers from three mice per group after 8 weeks. To control for loading, the blot was stripped and reprobed for β-actin. (**e**) Apoptosis of hepatocytes was evaluated by TUNEL staining of liver sections after 8 weeks of treatment. Photomicrographs from representative mice are shown. Morphometric analysis of TUNEL-stained sections from each MCD diet-fed group ($n = 5$ per group) at 8 weeks. Results are expressed as % of nuclei staining (+) for TUNEL (*$P < 0.05$).

steatohepatitis.[2] We focused on the role of IL-6 as a pro-inflammatory cytokine and used an inhibitor of the IL-6 receptor, MR16-1, in an MCD diet-induced NASH model, because an MCD diet was found to increase plasma IL-6 levels significantly and to activate hepatic IL6/GP130-related gene expression. Consequently, treatment of these mice with MR16-1 enhanced hepatic steatosis but ameliorated liver cell injury.

These contrasting observations regarding hepatic steatosis and inflammation indicate a paradoxical role for IL-6 in the development of chronic steatosis and inflammation of the liver. Recently, Horiguchi *et al* reported that, although STAT3 in hepatocytes, which depends on IL-6, could contribute to promote liver inflammation but inhibit steatosis by inhibiting SREBP-1 expression directly, STAT3 in macrophages/Kupffer cells, which depends on IL-10, could suppress liver inflammation during alcoholic liver injury.[29] This report reinforces our results. In our study, MR16-1 treatment blocked the MCD diet-induced hepatic STAT3 activation (Figure 2b) and ameliorated liver cell injury (Figure 6a). Interestingly, MR16-1 treatment also induced greater hepatic steatosis accompanied by increased hepatic SRBP-1 expression (Figures 3a and 4a). Further study regarding STAT3 activation in isolated hepatic macrophages/Kupffer cells obtained from MCD-diet fed mice and the effects of IL-10 is recommended in the future.

The role of IL-6 in the pathogenesis of NAFLD has been an issue of debate. Although IL-6 is well known as one of several proinflammatory cytokines active during infection, cahexia and obesity, IL-6 also is protective against various forms of liver damage.[4–7,10–17] According to the paper by Wallenius *et al*,[31] IL-6-deficient mice develop mature-onset obesity, which is reversed by IL-6 replacement. This finding is interesting and also reinforces our data that blocking IL-6/GP130

signaling deteriorates hepatic steatosis in MCD-diet induced NASH model. Therefore, the therapeutic use of IL-6/GP130 signaling in treating obesity seems to be an attractive target of future investigation. Recently, however, elevated proinflammatory cytokines have been shown in mice with obesity-related NASH.[9] These increased cytokines are believed to downregulate insulin signaling with increased SOCS3 protein in the liver.[32,33] Some other previous reports have also shown that long-term IL-6 exposure induced SOCS3 expression, caused insulin resistance and exacerbated liver injury, whereas short-term IL-6 exposure prevented hepatocyte apoptosis and steatosis after CCl4 treatment or partial hepatectomy.[34,35] Hence, we hypothesized that continuous IL-6 stimulation induced liver inflammation and fibrosis.

An MCD diet is believed to induce accumulation of hepatic triglycerides by inhibiting mitochondrial β-oxidation of fatty acids and blocking hepatic export of VLDL.[25] Unlike high-fat diets, which produce relatively little hepatic necroinflammation and fibrosis, MCD diets are used widely to induce NASH with fibrosis. Although an MCD diet inhibits mitochondrial oxidation of FA, thereby limiting that process as a source of ROS, this diet induces microsomal FA-oxidizing enzymes, such as Cyp2E1. The latter may produce sufficient ROS to trigger the secondary 'hits' that are required for progression from NAFLD to more advanced stages of fatty liver disease.[36,37] Thus, MCD diets promote NASH with fibrosis, even in nonobese mice. Moreover, recent interesting reports have shown that not only decreased VLDL secretion but also increased fatty acid uptake and cytoplasmic fatty acid synthesis genes, despite decreased nuclear levels of lipogenic transcription factors, such as SREBP-1, are the major mechanisms by which the MCD diet promotes intrahepatic lipid accumulation.[38] These discrepancies in lipogenic gene expression between the nuclei and cytoplasm seem to be present at an earlier stage of MCD diet-induced NASH. In this study, an MCD diet for 8 weeks decreased all lipogenic gene expression, mRNA levels of SREBPs, Acetyl-CoA Carboxylase, ATP-citrate lyase, fatty acid synthase and Stearoyl-CoA desaturase-1 and protein levels of PPARα in the liver (data not shown).

An MCD diet increased hepatic AMPK phosphorylation (Figure 1b). An MCD diet itself inhibits mitochondrial import of carnitine, thereby limiting FA oxidation that normally generates ATP. ROS/lipid peroxidation that results from alternative FA-oxidizing mechanisms also damages the mitochondria, further limiting ATP production. Gradual diet-related depletion of liver ATP pools activates AMPK. Furthermore, IL-6 also increases AMPK rapidly and markedly.[39,40] AMPK regulates the expression of genes involved in lipogenesis and mitochondrial biogenesis and also inhibits cell survival by binding to and phosphorylating insulin receptor substrate (IRS)-1 at Ser794.[40] Phosphorylation of IRS-1 at this site inhibits phosphatidylinositol 3-kinase/Akt signaling, suppresses the mitochondrial membrane potential and promotes apoptosis. In this model, Akt signaling was considered to be inhibited by increased AMPK and STAT3-induced SOCS3.[11] Hence, it can be postulated that MR16-1 treatment contributed to the recovery of Akt activity, resulting in reduced hepatocyte apoptosis in this model.

In conclusion, MR16-1 treatment decreased SOCS3 expression successfully, suppressed STAT3 activation and improved plasma FFA elevation through increased fatty acid uptake and hepatic triglyceride biosynthesis, leading to decreased Cyp2E1 expression, ROS production and hepatic apoptosis. As shown by our previous study, hepatic triglyceride synthesis may have a compensatory role for an impaired mechanism of FFA detoxification.[25] In clinical trial with neutralizing IL-6 receptor antibody, it was reported that plasma triglyceride and cholesterol levels were elevated in treated patients with rheumatoid arthritis.[21,41] It is interesting and necessary to investigate whether hepatic steatosis in those patients is ameliorated or exacerbated. Hopefully, further experiments using MR16-1 in other NASH models will show the effect of neutralizing IL-6 receptor on the hepatic histology in NASH.

Supplementary Information accompanies the paper on the Laboratory Investigation website (http://www.laboratoryinvestigation.org)

ACKNOWLEDGEMENT

This study was supported by a Grant-in-Aid for Scientific Research from the Japan Society for the Program of Science (Kanji Yamaguchi).

DISCLOSURE/CONFLICT OF INTEREST

The authors declare no conflict of interest.

1. Ludwig J, Viggiano TR, McGill DB, *et al.* Nonalcoholic steatohepatitis: Mayo Clinic experience with a hitherto unnamed disease.. Mayo Clin Proc 1980;55:434–438.
2. Day CP, James OF. Steatohepatitis: a tale of two 'hit'? Gastroenterology 1998;114:842–845.
3. Baranova A, Schlauch K, Elariny H, *et al.* Gene expression patterns in hepatic tissue and visceral adipose tissue of patients with non-alcoholic fatty liver disease. Obes Surg 2007;17:1111–1118.
4. Jarrar MH, Baranova A, Collantes R, *et al.* Adipokines and cytokines in non-alcoholic fatty liver disease. Aliment Pharmacol Ther 2008;27:412–421.
5. Diehl AM. Tumor necrosis factor and its potential role in insulin resistance and nonalcoholic fatty liver disease. Clin Liver Dis 2004;8:619–638.
6. Cressman DE, Greenbaum LE, DeAngelis RA, *et al.* Liver failure and defective hepatocyte regeneration in interleukin-6-deficient mice. Science 1996;274:1379–1383.
7. Selzner N, Selzner M, Odermatt B, *et al.* ICAM-1 triggers liver regeneration through TNF and IL-6 release in mice. Gastroenterology 2003;124:692–700.
8. Anty R, Bekri S, Luciani N, *et al.* The inflammatory C-reactive protein is increased in both liver and adipose tissue in severely obese patients independently from metabolic syndrome, type 2 diabetes, and NASH. Am J Gastroenterol 2006;101:1824–1833.
9. Wieckowska A, Papouchado BG, Li Z, *et al.* Increased hepatic and circulating interleukin-6 levels in human nonalcoholic steatohepatitis. Am J Gastroenterol 2008;103:1372–1379.
10. Febbraio MA. Gp130 receptor ligands as potential therapeutic targets for obesity. J Clin Invest 2007;117:841–849.
11. Inoue H, Ogawa W, Ozaki M, *et al.* Role of STAT-3 in regulation of hepatic gluconeogenic genes and carbohydrate metabolism *in vivo*. Nat Med 2004;10:168–174.

12. Peters M, Blinn G, Jostock T, *et al.* Combined interleukin 6 and soluble interleukin 6 receptor accelerates murine liver regeneration. Gastroenterology 2000;119:1663–1671.
13. Klein C, Wüstefeld T, Assmus U, *et al.* The IL-6-gp130-STAT3 pathway in hepatocytes triggers liver protection in T cell-mediated liver injury. J Clin Invest 2005;115:860–869.
14. Kovalovich K, Li W, DeAngelis R, *et al.* Interleukin-6 protects against Fas-mediated death by establishing a critical level of anti-apoptotic hepatic proteins FLIP, Bcl-2, and Bcl-xl. J Biol Chem 2001;276: 26605–26613.
15. Sun Z, Klein AS, Radaeva S, *et al. In vitro* interleukin-6 treatment prevents mortality associated with fatty liver transplants in rats. Gastroenterology 2003;125:202–215.
16. Jin X, Zhang Z, Beer-Stolz D, *et al.* Interleukin-6 inhibits oxidative injury and necrosis after extreme liver resection. Hepatology 2007;46:802–812.
17. Ramsay AJ, Husband AJ, Ramshaw IA, *et al.* The role of interleukin-6 in mucosal IgA antibody responses *in vivo*. Science 1994;264:561–563.
18. Selzner N, Selzner M, Jochum W, *et al.* Ischemic preconditioning protects the steatotic mouse liver against reperfusion injury: an ATP dependent mechanism. J Hepatol 2003;39:55–61.
19. Balkwill F, Mantovani A. Inflammation and cancer: back to Virchow? Lancet 2001;357:539–545.
20. Coussens LM, Werb Z. Inflammation and cancer. Nature 2002;420: 860–867.
21. Oldfield V, Dhillon S, Plosker GL. Tocilizumab: a review of its use in the management of rheumatoid arthritis. Drugs 2009;69:609–632.
22. Sahai A, Malladi P, Pan X, *et al.* Obese and diabetic db/db mice develop marked liver fibrosis in a model of nonalcoholic steatohepatitis: role of short-form leptin receptors and osteopontin. Am J Physiol Gastrointest Liver Physiol 2004;287:G1035–G1043.
23. Okazaki M, Yamada Y, Nishimoto N, *et al.* Characterization of anti-mouse interleukin-6 receptor antibody. Immunol Lett 2002;84:231–240.
24. Izumi-Nagai K, Nagai N, Ozawa Y, *et al.* Interleukin-6 receptor-mediated activation of signal transducer and activator of transcription-3 (STAT3) promotes choroidal neovascularization. Am J Pathol 2007;170: 2149–2158.
25. Yamaguchi K, Yang L, McCall S, *et al.* Inhibiting triglyceride synthesis improves hepatic steatosis but exacerbates liver damage and fibrosis in obese mice with nonalcoholic steatohepatitis. Hepatology 2007;45:1366–1374.
26. Anstee QM, Goldin RD. Mouse models in non-alcoholic fatty liver disease and steatohepatitis research. Int J Exp Pathol 2006;87:1–16.
27. Ota T, Takamura T, Kurita S, *et al.* Insulin resistance accelerates a dietary rat model of nonalcoholic steatohepatitis. Gastroenterology 2007;132:282–293.
28. Uchiyama Y, Yoshida H, Koike N, *et al.* Anti-IL-6 receptor antibody increases blood IL-6 level via the blockade of IL-6 clearance, but not via the induction of IL-6 production. Int Immunopharmacol 2008;8:1595–1601.
29. Horiguchi N, Wang L, Mukhopadhyay P, *et al.* Cell type-dependent pro- and anti-inflammatory role of signal transducer and activator of transcription 3 in alcoholic liver injury. Gastroenterology 2008;134:1148–1158.
30. Brunt EM, Janney CG, Di Bisceglie AM, *et al.* Nonalcoholic steatohepatitis: a proposal for grading and staging the histological lesions. Am J Gastroenterol 1999;94:2467–2474.
31. Wallenius V, Wallenius K, Ahren B, *et al.* Interleukin-6-deficient mice develop mature-onset obesity. Nat Med 2002;8:75–79.
32. Senn JJ, Klover PJ, Nowak IA, *et al.* Suppressor of cytokine signaling-3, a potential mediator of interleukin-6-dependent insulin resistance in hepatocytes. J Biol Chem 2003;278:13740–13746.
33. Ueki K, Kondo T, Tseng YH, *et al.* Central role of suppressors of cytokine signaling proteins in hepatic steatosis, insulin resistance, and the metabolic syndrome in the mouse. Proc Natl Acad Sci 2004;101: 10422–10427.
34. Jin X, Zimmers TA, Perez EA, *et al.* Paradoxical effects of short- and long-term interleukin-6 exposure on liver injury and repair. Hepatology 2006;43:474–484.
35. Rotter Sopasakis V, Larsson BM, Johansson A, *et al.* Short-term infusion of interleukin-6 does not induce insulin resistance *in vivo* or impair insulin signalling in rats. Diabetologia 2004;47:1879–1887.
36. Rinella ME, Elias MS, Smolak RR, *et al.* Mechanisms of hepatic steatosis in mice fed a lipogenic methionine choline-deficient diet. J Lipid Res 2008;49:1068–1076.
37. Leclercq IA, Farrell GC, Field J, *et al.* CYP2E1 and CYP4A as microsomal catalysts of lipid peroxides in murine nonalcoholic steatohepatitis. J Clin Invest 2000;105:1067–1075.
38. Larter CZ, Yeh MM, Haigh WG, *et al.* Hepatic free fatty acids accumulate in experimental steatohepatitis: role of adaptive pathways. J Hepatol 2008;48:638–647.
39. Ruderman NB, Keller C, Richard AM, *et al.* Interleukin-6 regulation of AMP-activated protein kinase. Potential role in the systemic response to exercise and prevention of the metabolic syndrome. Diabetes 2006;55(Suppl 2):S48–S54. Review.
40. Tzatsos A, Tsichlis PN. Energy depletion inhibits phosphatidylinositol 3-kinase/Akt signaling and induces apoptosis via AMP-activated protein kinase-dependent phosphorylation of IRS-1 at Ser-794. J Biol Chem 2007;282:18069–18082.
41. Hashizume M, Yoshida H, Koike N, *et al.* Over-produced IL-6 decreases blood lipid levels via up-regulation of VLDLR. Ann Rheum Dis 2010;69:741–746.

Hepatology Research

Hepatology Research 2010; 40: 654–660 doi: 10.1111/j.1872-034X.2010.00641.x

Case Report

Relapse of hepatitis C in a pegylated-interferon-α-2b plus ribavirin-treated sustained virological responder

Hideki Fujii,[1] Yoshito Itoh,[2] Naoki Ohnishi,[1] Masafumi Sakamoto,[1] Tohru Ohkawara,[1] Yoshihiko Sawa,[1] Koichi Nishida,[1] Takeshi Nishimura,[2] Kanji Yamaguchi,[2] Kohichiroh Yasui,[2] Masahito Minami,[2] Takeshi Okanoue,[3] Yasuo Ohkawara[1] and Toshikazu Yoshikawa[2]

[1]*Department of Internal Medicine, Aiseikai Yamashina Hospital,* [2]*Molecular Gastroenterology and Hepatology, Kyoto Prefectural University of Medicine, Graduate School of Medical Science, Kyoto, and* [3]*Division of Gastroenterology, Saiseikai Suita Hospital, Osaka, Japan*

A 41-year-old woman with chronic hepatitis C was treated with pegylated-interferon (PEG-IFN)-α-2b plus ribavirin for 24 weeks. She had hepatitis C virus (HCV) genotype 2a (1600 KIU/mL), and her liver histology showed mild inflammation and fibrosis. Four weeks after the start of the therapy, she achieved a rapid virological response (RVR) and then a sustained virological response (SVR). Serum alanine aminotransferase (ALT) levels remained within normal ranges and HCV RNA continued to be negative. However, ALT levels flared with the re-emergence of HCV RNA in the serum 1.5 years after discontinuation of therapy. HCV RNA obtained from sera before therapy and after relapse shared a 98.6% homology with the E2 region, and phylogenetic analyses indicated that they were the same HCV strain. These results eliminated the possibility of a re-infection and strongly indicated a late relapse of the disease. Therefore, follow-up is necessary for chronic hepatitis C patients after SVR, even if they respond well to therapy, including RVR.

Key words: chronic hepatitis C, genotype 2a, sustained virological response, relapse, phylogenetic analyses.

INTRODUCTION

HEPATITIS C VIRUS (HCV) is an important cause of chronic liver disease, and more than 170 million people are infected worldwide, including 1.5–2 million people in Japan.[1] Approximately 70% of Japanese chronic hepatitis C patients are infected with genotype 1b, whereas the rest are infected with genotypes 2a or 2b.[2] At present, pegylated-interferon (PEG-IFN)-α plus ribavirin is the optimal therapy for chronic hepatitis C. Sustained virological response (SVR), defined as undetectable serum HCV RNA 24 weeks after therapy completion, is the primary goal of this therapy. Approximately 80% of patients infected with genotypes 2 or 3 achieve SVR after 24 weeks of treatment, whereas approximately 50% patients with genotype 1 achieve SVR after 48 weeks of treatment.

Late relapse, defined as a HCV RNA reappearance in serum after achieving SVR, is rare in SVR patients. Furthermore, distinguishing relapse from re-infection is difficult without comparing the HCV nucleotide sequence before the start of the therapy and after relapse. Here we describe the clinical course of an HCV genotype 2a-infected woman treated with PEG-IFN-α plus ribavirin for 24 weeks. She achieved a rapid virological response (RVR) because HCV RNA was undetectable by a qualitative polymerase chain reaction (PCR) assay 4 weeks after initiating therapy. However, she achieved SVR and suffered a relapse of chronic hepatitis C 1.5 years after therapy discontinuation. We analyzed nucleotide sequences within the E2 region of HCV RNA containing the hypervariable region (HVR)1 and the IFN sensitivity-determining region (ISDR) of nonstructural protein 5A (NS5A), using sera before treatment and after relapse and confirmed that they were the same HCV strain.

Correspondence: Dr Yoshito Itoh, Molecular Gastroenterology and Hepatology, Kyoto Prefectural University of Medicine, 465 Kajii-cho, Kawaramachi-Hirokoji, Kamigyou-ku, Kyoto 602-8566, Japan. Email: yitoh@koto.kpu-m.ac.jp

Received 15 September 2009; revision 23 November 2009; accepted 6 December 2009.

CASE REPORT

A 41-YEAR-OLD WOMAN had elevated serum alanine aminotransferase (ALT; 138 IU/L) and aspartate aminotransferase (AST; 248 IU/L) levels on a routine medical check-up in mid-September 2005. Because of liver dysfunction in October 2005, she visited Aiseikai Yamashina General Hospital for further examination. She had no family history of liver diseases. Her height was 145 cm and weight was 42 kg. No abnormalities were detected on physical examination; her average alcohol intake was less than 20 g/week. She had no history of i.v. drug abuse.

Table 1 shows the laboratory data. On 25 October 2005, transaminase and biliary enzyme levels were elevated. Serum anti-HCV antibody was positive. The HCV RNA load was 2400 KIU/mL (Amplicor Monitor ver. 2.0; Roche Diagnostic Systems, Tokyo, Japan), and she had the 2a HCV genotype. She hesitated to undergo IFN treatment in the beginning. We strictly prohibited her from alcohol and started treating her with 600 mg/day oral ursodeoxycholic acid (UDCA) and 40 mL i.v. glycyrrhizin twice a week (Stronger Neo-Minophagen C, SNMC). Her liver functions improved significantly, but did not normalize following treatment with UDCA and SNMC.

She was admitted to Aiseikai Yamashina General Hospital on 3 February 2006, and PEG-IFN plus ribavirin treatment was initiated for chronic hepatitis C. Abdominal ultrasonography revealed that the liver was almost normal in size, the edge was sharp and the internal echo was slightly coarse. Other tests including hepatitis B virus PCR, HBc antibody, HIV 1/2 antibodies, antinuclear antibody, anti-mitochondrial antibody, serum ceruloplasmin, copper and ferritin were normal. The laboratory test results obtained on 3 February 2006 are presented in Table 1. The liver biopsy specimen before treatment revealed mild fibrosis with mild inflammation, which was graded as A1F1 according to the classification of Ichida *et al.* or Bedossa and Poynard.[3,4] She received combination therapy consisting of PEG-IFN-α-2b (1.5 μg/kg; 60 μg) once a week plus 600 mg ribavirin daily.

After therapy initiation, ALT levels declined rapidly and remained within the normal range after completion of the treatment. Serum HCV RNA levels were measured by a quantitative PCR assay (Amplicor HCV Monitor ver. 2.0) before therapy initiation and after relapse and by a qualitative PCR assay (Amplicor HCV Test ver. 2.0) at 4, 8, 12, 16, 20 and 24 weeks (all during the treatment period) as well as at 4, 8, 12, 16, 20 and 24 weeks after therapy completion. Serum HCV RNA was qualitatively

Table 1 Laboratory findings

	Normal	Initial visit (10/20/2005)	Before PEG-IFN + Rib (2/3/2006)	After relapse (1/25/2008)
White blood cell (μL)	(3900–9300)	9070	8110	8800
Red blood cell ($\times10^4$/μl)	(425–571)	458	433	412
Platelet ($\times10^4$/μL)	(12.7–35.6)	29.2	29.7	27.3
PT (%)		85%	82%	92%
Albumin (g/dL)	(4.0–5.0)	4.2	4.2	4.1
T. Bil (mg/dL)	(0.3–1.2)	0.6	0.4	0.4
AST (IU/l)	(<33)	87	35	61
ALT (IU/l)	(<35)	195	38	96
ALP (IU/l)	(115–360)	278	240	247
γ-GTP (IU/l)	(<47)	256	48	88
RPR	(–)	NA	(–)	(–)
HBsAg	(–)	(–)	(–)	(–)
ANA	(<40)	NA	<40	<40
Type IV collagen 7S (ng/mL)	(<5)	NA	3.8	3.2
Serum ferritin (ng/mL)	(5.3–179.7)	NA	50.7	NA
HCV RNA (Amplicor Monitor ver. 2.0) (KIU/mL)	(–)	2400	1600	2600
HCV genotype		2a	2a	2a

ALP, alkaline phosphatase; ALT, alanine aminotransferase; ANA, antinuclear antibody; AST, aspirate aminotransferase; γ-GTP, γ-glutamyltranspeptidase; HBsAg, hepatitis B surface antigen; HCV, hepatitis C virus; NA, not available; PT, prothrombin time; RPR, Rapid Plasma Reagin; T. Bil., total bilirubin.

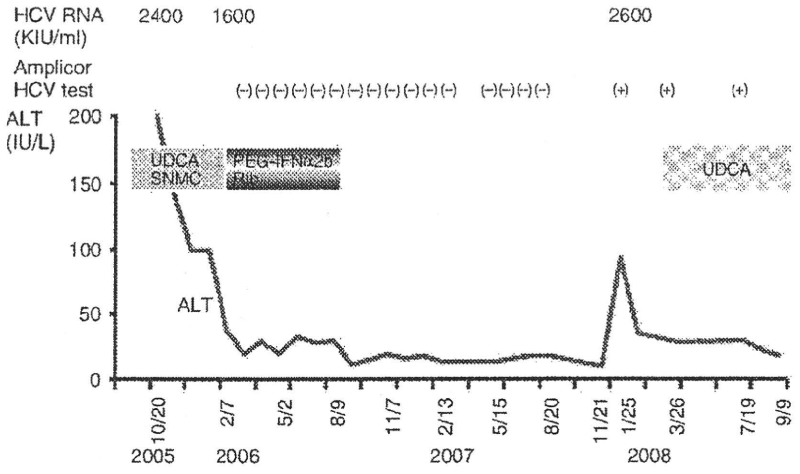

Figure 1 Levels of alanine aminotransferase (ALT) and hepatitis C virus (HCV) RNA load during the clinical course. Pegylated-interferon (PEG-IFN)-α plus ribavirin combination therapy was started in February 2006 and continued for 24 weeks until August 2006. HCV RNA was undetectable within 4 weeks. ALT levels remained within normal ranges until November 2007. Relapse occurred in January 2008. SNMC, Stronger Neo-Minophagen C; UDCA, ursodeoxycholic acid.

undetectable 4 weeks after therapy initiation and remained undetectable 6 months after therapy completion. The patient had few side-effects, and the treatment was completed without reducing either of the drugs.

After achieving SVR, she underwent monthly liver function tests, and a qualitative PCR assay was performed occasionally. In December 2007, her liver function tests deteriorated. AST/ALT levels were elevated, and she tested positive for HCV RNA on 25 January 2008 (Fig. 1, Table 1). A quantitative PCR assay indicated that the HCV RNA titer was 2600 IU/L, and the HCV genotype was 2a. The patient again started taking 600 mg UDCA daily, and ALT returned to low levels (~30–40 IU/L). Repeated tests showed that HCV RNA was persistently positive.

To determine if HCV RNA that appeared 1.5 years after treatment completion was identical to that before therapy, we compared the nucleotide sequences of the two coding regions, namely, the E2 region containing HVR1 and ISDR of NS5A. Informed consent was obtained from the patient before analysis, and the serum samples obtained before treatment and after relapse were stored at −80 °C until use.

Virological analyses proceeded as follows. To reconfirm HCV genotyping, direct sequencing of the 5′-untranslated region was performed, as described previously.[5,6] The genotypes were classified according to the nomenclature proposed in a previous report and were determined to be 2a in both the samples. HCV RNA was amplified by reverse transcription (RT)–PCR to directly sequence the E2 and ISDR regions.

In brief, RNA was extracted from 140 μL sera using a commercially available kit (QIAamp viral RNA kit; QIAGEN, Valencia, CA, USA) and dissolved in 50 μL diethylpyrocarbonate-treated water. This sample was used for RT with random hexamer primers (SuperScript III First-Strand Synthesis System for RT–PCR cDNA synthesis kit; Invitrogen, Carlsbad, CA, USA). The E2 region was amplified by nested PCR, and ISDR regions were amplified by hemi-nested PCR. Each 50-μL PCR reaction contained 100 nM of each primer, 1 ng template cDNA, 5 μL 10× Ex Taq buffer, 4 μL deoxyribonucleotide triphosphate mixture, and 1.25 U of Takara Ex Taq HS (Takara Ex Taq, Otsu, Japan).

The PCR primers were set based on a reference HCV sequence (accession no. AF177036).

The first PCR primer sequences for E2 were: sense (1422, 1441) 5′-ACTTCTCTATGCAGGGAGCG-3′ and antisense (2437, 2418) 5′-GTTTTGGTGGAGGTGGAG AA-3′; and sense (2171, 2190) 5′-TGCCTGATCGACTA CCCCTA-3′ and antisense (2730, 2711) 5′-AGGCC AGTGAGGGAATAGGT-3′. The second PCR primer sequences for E2 were: sense (1453, 1472) 5′-CGTT GTCATCCTTCTGTTGG-3′ and antisense (2261, 2242) 5′-CAACCCCTCCCACATACATC-3′; and sense (2189, 2208) 5′-TACAGGCTCTGGCATTACCC-3′ antisense (2698, 2679) 5′-TACCCGACCCTTGATGTACC-3′.

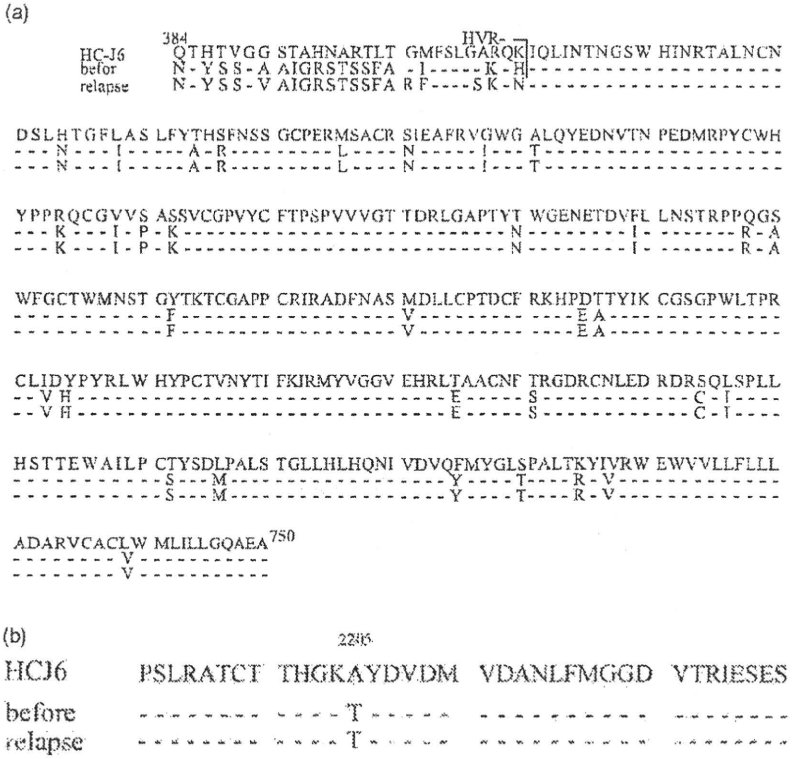

Figure 2 (a) Comparison of the hepatitis C virus (HCV) E2 (top) region amino acid sequences. Sequencing was performed for serum samples obtained before therapy on 3 February 2006 and after relapse on 25 January 2008. Sequences were aligned against the HCJ6 HCV genotype 2a reference sequence (GenBank accession no. D00944). Hypervariable region (HVR)1 positions of E2 are indicated by numbers corresponding to the amino acid positions within the HCV genotype 2a polyprotein of the reference sequence. There were five amino acid mutations in these regions between the two samples. (b) IFN sensitivity-determining region (ISDR) sequences before therapy and after relapse showed the same single mutation at codon 2205. Sequences were aligned against the HCJ6 HCV genotype 2a reference sequence (GenBank accession no. D00944). ISDR positions are indicated as numbers corresponding to the amino acid positions within the HCV genotype 2a polyprotein of the reference sequence.

The first PCR primer sequences for ISDR were: sense (6866, 6885) 5′-ACGTCCATGCTAACAGACCC-3′ and antisense (7185, 7166) 5′-GGGAATCTCTTCTTGGG GAG-3′. The second PCR primer sequences for ISDR were the sense primer from the first-round PCR and a new antisense primer (7109, 7090) 5′-CGAGAG AGTCCAGAACGACC-3′.[7]

Polymerase chain reaction products were separated by electrophoresis on 1% or 2% agarose gels, stained with ethidium bromide, and visualized under ultraviolet light. The products were purified and sequenced with second-round PCR primers, using a dye terminator sequencing kit (BigDye Terminator ver. 1.1 cycle sequencing kit; Applied Biosystems, Foster City, CA, USA) and an ABI PRISM 310 genetic analyzer (Applied Biosystems). Sequence alignments and phylogenetic analyses were performed with MEGA4 software.[8] Nucleotide sequences obtained from the two samples were compared to 23 published HCV genotype 2a sequences. A phylogenetic tree was constructed by the neighbor-joining method[9] based on the nucleotide sequence of the E2 region, with pairwise distances being estimated using the Kimura two-parameter method. Bootstrap values were determined on 1000 re-samplings of data sets.[10]

The E2 nucleotide sequences before treatment and after relapse were 98.6% similar. Except HVR1, two of the samples were 99.0% similar. The amino acid sequences in the E2 region, except HVR1, were identical between the two samples. There was a difference of five amino acids in HVR1 (Fig. 2a).

When compared to known HCV isolates of various genotypes whose entire coding region sequence has

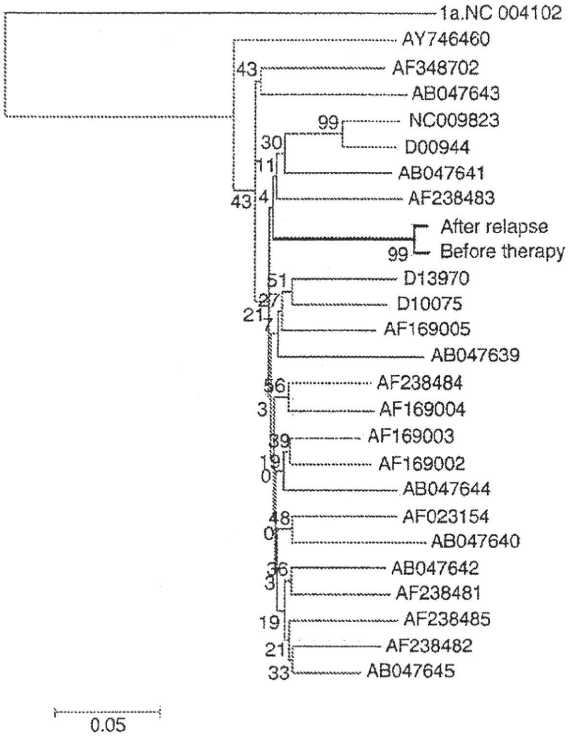

Figure 3 A phylogenetic tree was constructed by the neighbor-joining method based on the nucleotide sequence of the E2 region (1101 nt) of 23 genotype 2a strains using the genotype 1a hepatitis C virus (HCV) isolate (NC004102) as an outgroup. The isolates obtained in the present study before therapy and after relapse are indicated in bold letters for clarity. Twenty-three reported genotype 2a HCV isolates, whose entire coding region sequence is known, are included for comparison, and their accession numbers are shown. Bootstrap values were determined on 1000 re-samplings of datasets.

been determined, the two isolates were the closest to a particular genotype 2a HCV isolate (accession no. AB047645) with 87.3% nucleotide sequence similarity; however, the isolates were only 64.4–72.7% similar to known genotype non 2a (1a NC004102, 1b D90208, 2b D01221, 3a D17763, 4a Y11604, 5a Y13184 and 6a Y12083). The phylogenetic tree of 23 genotype 2a HCV isolates, constructed based on the E2 1101-nucleotide sequence, indicated that the sample obtained after relapse bifurcated from a common trunk with the sample before treatment, and we confirmed that these two samples were the closest to each other among all known genotype 2a HCV isolates (Fig. 3). The results of sequencing analysis before therapy and after re-emergence of viremia ruled out the possibility of a re-infection and strongly suggested a late relapse of chronic hepatitis C.

Interferon sensitivity-determining region sequences before treatment and after relapse showed 98.9% similarity. The amino acid sequences of the two ISDR regions were completely identical. The sequences of the HCJ6 (accession no. D00944) strain were defined as wild-type ISDR, and those that deviated from this strain were defined as the mutant type. ISDR sequences before treatment and after relapse were different in only one codon (2205) when compared with the reference HCJ6 sequence (Fig. 2b).

DISCUSSION

IN THIS STUDY, we clarified that E2 1101-nucleotide sequences of HCV isolated from sera before treatment and after relapse shared a 98.6% homology. Furthermore, phylogenetic analyses classified these two samples as the same strain. These results ruled out the possibility of a re-infection and strongly suggested a late relapse of chronic hepatitis C.

Hepatitis C virus is an RNA virus belonging to the genus *Hepacivirus* in the Flaviviridae family. Similar to other RNA viruses, HCV circulates as a genetically distinct population, demonstrating a quasispecies.[11] HCV HVR1, which is composed of 27 amino acids and is located at the 5′ terminus of the E2 gene, is highly variable among and within infected patients,[12–14] so it can be used to identify individual HCV isolates.[15,16] HCV HVR1 changes rapidly over time in the same individual. Our pairwise sequences were not completely identical but shared a high homology, which was equal to the homology reported previously.[16] These results suggest that the patient achieved SVR but suffered a relapse of hepatitis C after 1.5 years.

Some reports have indicated that in a majority of patients with SVR, low-level HCV RNA can be detected in lymphocytes, monocytes/macrophages and liver, despite constantly undetectable HCV RNA in sera.[17–19] This "occult" persistence of HCV replication could potentially play a role in late recurrence after treatment. However, the significance/mechanism of HCV RNA persistence in the liver or peripheral blood mononuclear cells is still uncertain, and data regarding occult persistence are conflicting.[20] Moreover, it is unclear as to how many of these late relapse patients were "true" relapsers and how many were re-infected. The relapse rates after SVR in IFN monotherapy are approximately 5–10%.[21,22] Nakayama *et al.* recently reported a late relapse of

hepatitis C after IFN-α plus ribavirin therapy and summarized late relapsing cases in Japan.[23] They indicated that compared to reports from foreign countries, late relapses were very rare in Japan, particularly after IFN and ribavirin therapy and that the relapse interval was principally restricted to within 2 years after therapy completion. Four hundred and fifty-five chronic hepatitis C patients were cured by PEG-IFN plus ribavirin therapy in the study group of Kyoto Prefectural University of Medicine and related hospitals, and this is the only case of late relapse to date (Itoh Y. *et al.*, 2009 unpublished data). This may be the first reported case of relapse after SVR with PEG-IFN plus ribavirin therapy.

Several host and viral characteristics are associated with the likelihood of response to IFN-based therapy. The HCV genotype and viral load are the most important viral predictors, and the ISDR sequence variation[24] and substitutions of amino acids 70 and/or 91 in the core region[25] within the HCV genome have been recently advocated in patients with genotype 1. It is interesting to note that only one amino acid varied in ISDR compared to the reference sequence in our case. For patients with HCV genotype 2a, Hayashi *et al.* reported that ISDR amino acid variations compared to the reference sequence and RVR as well as negative HCV at 4 weeks are important predictors of SVR in PEG-IFN monotherapy.[7] ISDR interacts with interferon-inducible double-stranded RNA-activated protein kinase (PKR) and inactivates HCV replication *in vitro*.[26] According to the report by Hayashi *et al.*,[7] an A-to-T mutation at codon 2205 (Fig. 2b) can be interpreted as wild type, and hence ISDR in this case contained no mutations, which may have influenced HCV RNA re-emergence after achieving SVR.

Patients with RVR, defined as a negative HCV RNA at 4 weeks, are more likely to have SVR.[7,27] In our case, HCV RNA was negative at 4 weeks, which indicated that this case may be cured; however, relapse of hepatitis C occurred after 1.5 years. The data concerning the efficacy of re-treatment of genotype 2 chronic hepatitis C are limited. According to the report by Moucari *et al.*,[28] there is a higher rate of SVR in genotype non-1 relapsers. Therefore, our patient could be retreated with a second PEG-IFN plus ribavirin combination therapy. However, because the patient is 41 years old and has stage F1 hepatic fibrosis, we will recommend that she wait for a new drug such as a protease inhibitor. Further research for unknown factors to predict late relapse after achieving SVR might be necessary.

In conclusion, SVR patients may have a potential risk of HCV reactivation. Annual surveillance including HCV RNA testing seems clinically reasonable for detecting spontaneous relapse and recurrence of hepatitis C in SVR patients.

REFERENCES

1 National Institutes of Health Consensus Development Conference Statement: Management of hepatitis C: 2002 – June 10–12, 2002. *Hepatology* 2002; 36: S3–20.
2 Hayashi J, Kishihara Y, Yamaji K *et al.* Transmission of hepatitis C virus by health care workers in a rural area of Japan. *Am J Gastroenterol* 1995; 90: 794–9.
3 Ichida F, Tsuji T, Omata M *et al.* New Inuyama classification: new criteria for histological assessment of chronic hepatitis. *Internat Hepatol Comm* 1996; 6: 112–9.
4 Bedossa P, Poynard T. An algorithm for the grading of activity in chronic hepatitis C. The METAVIR Cooperative Study Group. *Hepatology* 1996; 24: 289–93.
5 Germer JJ, Rys PN, Thorvilson JN, Persing DH. Determination of hepatitis C virus genotype by direct sequence analysis of products generated with the Amplicor HCV test. *J Clin Microbiol* 1999; 37: 2625–30.
6 Gargiulo F, De Francesco MA, Pinsi G *et al.* Determination of HCV genotype by direct sequence analysis of quantitative PCR products. *J Med Virol* 2003; 69: 202–6.
7 Hayashi K, Katano Y, Honda T *et al.* Mutations in the interferon sensitivity-determining region of hepatitis C virus genotype 2a correlate with response to pegylated-interferon-alpha 2a monotherapy. *J Med Virol* 2009; 81: 459–66.
8 Tamura K, Dudley J, Nei M, Kumar S. MEGA4: Molecular Evolutionary Genetics Analysis (MEGA) software version 4.0. *Mol Biol Evol* 2007; 24: 1596–9.
9 Saitou N, Nei M. The neighbor-joining method: a new method for reconstructing phylogenetic trees. *Mol Biol Evol* 1987; 4: 406–25.
10 Felsenstein J. Confidence limits on phylogenies: An approach using the bootstrap. *Evolution* 1985; 39: 783–91.
11 Martell M, Esteban JI, Quer J *et al.* Hepatitis C virus (HCV) circulates as a population of different but closely related genomes: quasispecies nature of HCV genome distribution. *J Virol* 1992; 66: 3225–9.
12 Ogata N, Alter HJ, Miller RH, Purcell RH. Nucleotide sequence and mutation rate of the H strain of hepatitis C virus. *Proc Natl Acad Sci USA* 1991; 88: 3392–6.
13 Weiner AJ, Geysen HM, Christopherson C *et al.* Evidence for immune selection of hepatitis C virus (HCV) putative envelope glycoprotein variants: potential role in chronic HCV infections. *Proc Natl Acad Sci USA* 1992; 89: 3468–72.
14 Okamoto H, Kojima M, Okada S *et al.* Genetic drift of hepatitis C virus during an 8.2-year infection in a chimpanzee: variability and stability. *Virology* 1992; 190: 894–9.
15 Lee WM, Polson JE, Carney DS, Sahin B, Gale M Jr. Reemergence of hepatitis C virus after 8.5 years in a patient with

hypogammaglobulinemia: evidence for an occult viral reservoir. *J Infect Dis* 2005; 192: 1088–92.
16 Nakayama H, Sugai Y, Ikeya S, Inoue J, Nishizawa T, Okamoto H. Molecular investigation of interspousal transmission of hepatitis C virus in two Japanese patients who acquired acute hepatitis C after 40 or 42 years of marriage. *J Med Virol* 2005; 75: 258–66.
17 Castillo I, Rodriguez-Inigo E, Lopez-Alcorocho JM, Pardo M, Bartolome J, Carreno V. Hepatitis C virus replicates in the liver of patients who have a sustained response to antiviral treatment. *Clin Infect Dis* 2006; 43: 1277–83.
18 Pham TN, MacParland SA, Mulrooney PM, Cooksley H, Naoumov NV, Michalak TI. Hepatitis C virus persistence after spontaneous or treatment-induced resolution of hepatitis C. *J Virol* 2004; 78: 5867–74.
19 Radkowski M, Gallegos-Orozco JF, Jablonska J *et al.* Persistence of hepatitis C virus in patients successfully treated for chronic hepatitis C. *Hepatology* 2005; 41: 106–14.
20 Welker MW, Zeuzem S. Occult hepatitis C: how convincing are the current data? *Hepatology* 2009; 49: 665–75.
21 McHutchison JG, Poynard T, Esteban-Mur R *et al.* Hepatic HCV RNA before and after treatment with interferon alone or combined with ribavirin. *Hepatology* 2002; 35: 688–93.
22 Veldt BJ, Saracco G, Boyer N *et al.* Long term clinical outcome of chronic hepatitis C patients with sustained virological response to interferon monotherapy. *Gut* 2004; 53: 1504–8.
23 Nakayama H, Ojima T, Kusano M, Endo K, Takahashi M, Sugai Y. Two cases of chronic hepatitis C with sustained virological response in whom serum HCV RNA reappeared two or twelve years after the end of IFN treatment. *Kanzo* 2006; 47: 550–7. (In Japanese).
24 Enomoto N, Sakuma I, Asahina Y *et al.* Mutations in the nonstructural protein 5A gene and response to interferon in patients with chronic hepatitis C virus 1b infection. *N Engl J Med* 1996; 334: 77–81.
25 Akuta N, Suzuki F, Sezaki H *et al.* Association of amino acid substitution pattern in core protein of hepatitis C virus genotype 1b high viral load and non-virological response to interferon-ribavirin combination therapy. *Intervirology* 2005; 48: 372–80.
26 Gale M Jr, Blakely CM, Kwieciszewski B *et al.* Control of PKR protein kinase by hepatitis C virus nonstructural 5A protein: molecular mechanisms of kinase regulation. *Mol Cell Biol* 1998; 18: 5208–18.
27 Shiffman ML, Suter F, Bacon BR *et al.* Peginterferon alfa-2a and ribavirin for 16 or 24 weeks in HCV genotype 2 or 3. *N Engl J Med* 2007; 357: 124–34.
28 Moucari R, Ripault MP, Oules V *et al.* High predictive value of early viral kinetics in retreatment with peginterferon and ribavirin of chronic hepatitis C patients non-responders to standard combination therapy. *J Hepatol* 2007; 46: 596–604.

Hepatology Research 2010; 40: 901–910 doi: 10.1111/j.1872-034X.2010.00704.x

Original Article

Lower circulating levels of dehydroepiandrosterone, independent of insulin resistance, is an important determinant of severity of non-alcoholic steatohepatitis in Japanese patients

Yoshio Sumida,[1] Yoshikazu Yonei,[2] Kazuyuki Kanemasa,[1] Tasuku Hara,[1] Yutaka Inada,[1] Kyoko Sakai,[1] Shunsuke Imai,[3] Sawako Hibino,[4] Kanji Yamaguchi,[5] Hironori Mitsuyoshi,[5] Kohichiroh Yasui,[5] Masahito Minami,[5] Yoshito Itoh,[5] Yuji Naito,[5] Toshikazu Yoshikawa[5] and Takeshi Okanoue[6]

[1]Center for Digestive and Liver Diseases, [3]Department of Pathology, Nara City Hospital, Nara, [2]Anti-Aging Medical Research Center, Graduate School of Life and Medical Science, Doshisha University, Kyotanabe, [4]Anti-Aging Medical Science, Division of Basic Research, Louis Pasteur Center for Medical Research, [5]Department of Gastroenterology and Hepatology, Kyoto Prefectural University of Medicine, Kyoto, and [6]Hepatology Center, Saiseikai Suita Hospital, Suita, Japan

Aim: The biological basis of variability in histological progression of non-alcoholic fatty liver disease (NAFLD) remains unknown. Dehydroepiandrosterone (DHEA), the most abundant steroid hormone, has been shown to influence sensitivity to reactive oxygen species, insulin sensitivity and expression of peroxisome proliferator-activated receptor-α. Our aim was to determine whether more histologically advanced NAFLD is associated with low circulating levels of DHEA in Japanese patients.

Methods: Serum samples were obtained in 133 Japanese patients with biopsy-proven NAFLD and in 399 sex- and age-matched healthy people undergoing health checkups. Serum levels of sulfated DHEA (DHEA-S) were measured by chemiluminescent enzyme immunoassay.

Results: Serum DHEA-S levels in NAFLD patients were similar to those in the control group. Of 133 patients, 90 patients were diagnosed as non-alcoholic steatohepatitis (NASH): 73 patients had stage 0–2, and 17 had stage 3 or 4. Patients with advanced NAFLD (NASH with fibrosis stage 3 or 4) had lower plasma levels of DHEA-S than patients with mild NAFLD (simple steatosis or NASH with fibrosis stage 0–2). The area under the receiver operating characteristic curve for DHEA in separating patients with and without advanced fibrosis was 0.788. A "dose effect" of lower DHEA-S and incremental fibrosis stage was observed with a mean DHEA-S of 170.4 ± 129.2, 137.6 ± 110.5, 96.2 ± 79.3, 61.2 ± 46.3 and 30.0 ± 32.0 μg/dL for fibrosis stages 0, 1, 2, 3, and 4, respectively. The association between DHEA-S and severity of NAFLD persisted after adjusting for age, sex and insulin resistance.

Conclusion: Low circulating DHEA-S might have a role in the development of advanced NASH.

Key words: fibrosis, dehydroepiandrosterone, insulin resistance, non-alcoholic fatty liver disease.

INTRODUCTION

NON-ALCOHOLIC FATTY LIVER disease (NAFLD) is the most common chronic liver disease in many developed countries and results in a serious public health problem worldwide. NAFLD includes a wide spectrum of liver diseases, ranging from simple steatosis (SS), which is usually a benign and non-progressive condition, to non-alcoholic steatohepatitis (NASH), which may progress to liver cirrhosis (LC) and hepatocellular carcinoma (HCC) in the absence of significant alcohol consumption.[1–3] In Japan, current best estimates make the prevalence of NAFLD approximately 20% and of NASH 2–3% in the general population.[4,5] Although several factors have been associated with more advanced NAFLD, the biological basis of the histological diversity of severity of NAFLD (i.e. why some patients develop

Correspondence: Dr Yoshio Sumida, Center for Digestive and Liver Diseases, Nara City Hospital, 1-50-1 Higashi Kidera-cho, Nara 630-8305, Japan. Email: sumida@nara-jadecom.jp
Received 9 April 2010; revision 2 June 2010; accepted 7 June 2010.

SS and others develop NASH with advanced fibrosis) remains unknown. More advanced NAFLD is characterized by insulin resistance,[6,7] oxidative stress[8,9] and advanced fibrosis.

Endocrine hormones control cell metabolism and the distribution of body fat and therefore may contribute to the development of NAFLD or NASH. It has been postulated that dehydroepiandrosterone (DHEA) and its sulfate ester, dehydroepiandrosterone sulfate (DHEA-S), the major secretory products of the human adrenal gland, may be discriminators of life expectancy and aging.[10] DHEA-S concentration is independently and inversely related to death from any cause and death from cardiovascular disease in men over the age of 50 years.[11] DHEA is a potential mediator of reactive oxygen species scavenger synthesis[12] and has also been reported to augment insulin sensitivity[13–16] and peroxisome proliferator activation.[17,18] Recently, Charlton *et al.* observed that levels of DHEA are significantly lower in patients with histologically advanced NASH, as compared with patients with mild NASH or SS.[19] DHEA levels exert a good sensitivity and specificity in discriminating patients with more advanced histological disease, as shown by receiver–operator curve (ROC) analysis.

To validate their results, we determined circulating DHEA levels in Japanese patients with biopsy-proven NAFLD.

METHODS

Patients

A TOTAL OF 133 patients with well-characterized and liver biopsy-confirmed NAFLD were included in this study. They were consecutively biopsied patients seen at the Center for Digestive and Liver Diseases, Nara City Hospital during 2007–2009. The diagnosis of NAFLD was based on the following criteria: (i) persistent elevations of transaminase activities for more than 6 months; (ii) liver biopsy showing steatosis in at least 5% of hepatocytes;[20] and (iii) appropriate exclusion of liver diseases of other etiology including viral hepatitis, autoimmune hepatitis, drug-induced liver disease, primary biliary cirrhosis (PBC), biliary obstruction, hemochromatosis, Wilson's disease, and α-1-antitrypsin-deficiency-associated liver disease. Patients consuming more than 20 g alcohol/day and patients with evidence of decompensated LC or HCC were excluded from the present study. Written informed consent was obtained from all patients at the time of their liver biopsy, and the study was conducted in conformance with the Helsinki Declaration. In addition, 399 sex- and age-matched healthy people participating in health checkups who showed normal levels of alanine aminotransferase (ALT) levels (≤30 IU/L) were also enrolled as the control group.

Clinical laboratory parameters

Venous blood samples were taken in the morning after a 12-h overnight fast. The laboratory evaluation in all patients included a blood cell count and the measurement of aspartate aminotransferase (AST), ALT, γ-glutamyltransferase (γGT), cholinesterase (ChE), total cholesterol, triglyceride, albumin, fasting plasma glucose (FPG), immunoreactive insulin (IRI), free fatty acid (FFA), ferritin levels, hyaluronic acid and type IV collagen 7S. These parameters were measured using the standard techniques of clinical chemistry laboratories. Body mass index (BMI) was calculated using the following formula: weight in kilograms / (height in meters).[2] Obesity was defined as a BMI greater than 25, according to the criteria of the Japan Society for the Study of Obesity.[21] Patients were assigned a diagnosis of diabetes mellitus (DM) if a documented use of oral hypoglycemic medication, a random glucose level in excess of 200 mg/dL or an FPG greater than 126 mg/dL was present.[22] Dyslipidemia was diagnosed if the cholesterol level was higher than 220 mg/dL and/or the triglyceride level was over 160 mg/dL. Hypertension was diagnosed if the patient was on antihypertensive medication and/or had a resting recumbent blood pressure of greater or equal to 140/90 mmHg on at least two occasions.

Sulfated DHEA concentrations were measured by chemiluminescent enzyme immunoassay (CLEIA). Serum DHEA-S levels of the control group were determined in the Anti-Aging Medical Research Center, Graduate School of Life and Medical Science, Doshisha University, Kyoto, Japan. The Homeostatic Model of Assessment of Insulin Resistance (HOMA-IR) was calculated on the basis of fasting values of plasma glucose and insulin according to the HOMA model formula: HOMA-IR = IRI (μU/mL) × FPG (mg/dL) / 405.[23] Quantitative insulin sensitivity check index (QUICKI) = 1 / (log fasting IRI [μU/mL] + log FPG [mg/dL]).[24]

Histological evaluation

All patients enrolled in this study underwent a percutaneous liver biopsy under ultrasonic guidance. The liver specimens were embedded in paraffin and stained with hematoxylin–eosin, Masson trichrome and reticulin

Table 1 Characteristics of NAFLD patients and control group

Parameters	NAFLD	Control	*P*-value
n	133	399	
Sex (female)	70 (53%)	210 (53%)	Matched
Age (year)	55.2 (15.4)	55.6 (12.1)	0.7990
BMI (kg/m^2)	27.9 (4.9)	23.4 (3.4)	<0.0001
Obesity (BMI > 25 kg/m^2)	98 (74%)	109 (27%)	<0.0001
AST (IU/L)	58.0 (33.0)	21.7 (4.9)	<0.0001
ALT (IU/L)	85.6 (51.7)	19.4 (5.4)	<0.0001
γGT (IU/L)	82.8 (73.0)	33.1 (28.8)	<0.0001
Cholesterol (mg/dL)	207.9 (41.2)	215.6 (34.9)	0.0572
Triglyceride (mg/dL)	179.1 (96.3)	109.0 (87.8)	<0.0001
HDL-C (mg/dL)	52.0 (24.7)	63.8 (16.6)	<0.0001
FPG (mg/dL)	103.5 (38.9)	97.5 (15.7)	0.0131
IRI (μU/mL)	14.70 (9.46)	5.57 (4.17)	<0.0001
HOMA-IR	3.93 (3.83)	1.37 (1.09)	<0.0001
QUICKI	0.33 (0.03)	0.38 (0.04)	<0.0001
DHEA-S (μg/dL)	128.7 (111.2)	113.6 (91.8)	0.1578

P-values were calculated by Student's *t*-test or χ^2-test analysis.
Results are presented as numbers with percentages in parenthesis for qualitative data or as means with standard deviation in parenthesis for quantitative data.
ALT, alanine aminotransferase; AST, aspartate aminotransferase; BMI, body mass index; DHEA-S, dehydroepiandrosterone sulfate; FPG, fasting plasma glucose; HDL-C, high-density lipoprotein cholesterol; HOMA-IR, Homeostasis Model Assessment for Insulin Resistance; IRI, immunoreactive insulin; NAFLD, non-alcoholic fatty liver disease; QUICKI, Quantitative insulin sensitivity check index; γGT, gamma glutamyl transpeptidase.

silver stain. A pathologist (S. I.) who was blinded to the clinical data reviewed the liver biopsy specimens. Adequate liver biopsy sample was defined as biopsy specimen length greater than 1.5 cm and/or having more than six portal tracts. NASH was defined as steatosis with lobular inflammation and ballooning degeneration with or without Mallory–Denk body or fibrosis.[2,3] Patients whose liver biopsy specimens showed steatosis, or steatosis with non-specific inflammation, were identified as the SS cohort.[2,3] The severity of hepatic fibrosis (stage) was defined as follows: stage 1, zone 3 perisinusoidal fibrosis; stage 2, zone 3 perisinusoidal fibrosis with portal fibrosis; stage 3, zone 3 perisinusoidal fibrosis and portal fibrosis with bridging fibrosis; and stage 4, cirrhosis.[25] Scoring of steatosis included both microvesicular and macrovesicular steatosis and was based on the percentage area of the parenchyma that was fatty. Mild was considered less than 33%, moderate 33–65% and advanced if greater than 66% was observed.[20]

Statistical analysis

Results are presented as the means and standard deviation (SD) for quantitative data or as numbers with percentages in parentheses for qualitative data. Statistical differences in quantitative data were determined using the Student's *t*-test (Table 1). Statistical differences among three groups for quantitative data were determined by one-way ANOVA with Scheffe's post-hoc test (Table 3). Fisher's exact probability test or χ^2-test analysis was used for qualitative data (Tables 1,3). Correlation coefficients were calculated by using Spearman's rank correlation analysis (Table 2). Multivariate analysis was performed by logistic regression analysis to identify variables independently associated with advanced stage of NASH (Table 4). To assess the accuracy of clinical scoring system in differentiating NASH from SS or advanced NAFLD from mild NAFLD, we calculated the sensitivity and the specificity for each value of each test and then constructed ROC by plotting the Se against the reverse Sp (1 – Sp) at each value (Fig. 1). The diagnostic performance of scoring systems was assessed by analysis of ROC. The most commonly used index of accuracy is the area under the ROC (AUC), with values close to 1.0 indicating high diagnostic accuracy (Table 4). The Youden index was used to identify the optimal cut-off points. Differences were considered statistically significant at all $P < 0.05$.

Table 2 Correlation between serum DHEA-S and clinical parameters in 133 patients with biopsy-proven NAFLD

Variables	Correlation coefficient	*P*-value
Age	−0.6982	<0.0001
Hemoglobin	0.4859	<0.0001
Platelet	0.3475	<0.0001
AST	−0.1988	0.0218
ALT	0.1733	0.0460
AST : ALT ratio	−0.5847	<0.0001
γGT	−0.0580	0.5092
Cholinesterase	0.3827	<0.0001
Albumin	0.4165	<0.0001
Prothrombin time	0.0767	0.4029
Cholesterol	0.1525	0.0820
Triglyceride	0.2037	0.0206
HDL-C	−0.2016	0.0033
FPG	−0.1386	0.1158
IRI	−0.0208	0.8138
HOMA-IR	−0.0545	0.5379
QUICKI	0.0545	0.5379
Free fatty acid ($n = 121$)	−0.1023	0.2644
Ferritin	0.0037	0.9666
Hyaluronic acid	−0.6408	<0.0001
Type IV collagen 7 s	−0.4477	<0.0001

P-values are based on Spearman's non-parametric correlation analysis.
ALT, alanine aminotransferase; AST, aspartate aminotransferase; DHEA-S, dehydroepiandrosterone sulfate; FPG, fasting plasma glucose; HDL-C, high-density lipoprotein cholesterol; HOMA-IR, Homeostasis Model Assessment for Insulin Resistance; IRI, immunoreactive insulin; NAFLD, non-alcoholic fatty liver disease; QUICKI, Quantitative insulin sensitivity check index; γGT, gamma glutamyl transpeptidase.

RESULTS

Patient demographics

TABLE 1 SUMMARIZES the clinical, laboratory and liver biopsy data of the patient population and the control group. NAFLD patients were predominantly obese, had higher levels of transaminase activities, γGT, triglyceride, FPG, IRI and insulin resistance, and had lower levels of high-density lipoprotein cholesterol (HDL-C). Serum levels of DHEA-S in NAFLD patients were not different from those in sex- and age-matched controls. In both groups, there were significant sex differences in serum levels of DHEA-S (control group, male 154.4 ± 102.1 vs female 76.8 ± 59.6 μg/dL, $P < 0.0001$; NAFLD group, male 186.7 ± 129. 2 vs female 76.5 ± 53.1 μg/dL, $P < 0.0001$).

Of 133 NAFLD patients involved in this study, 90 patients (68%) were histologically diagnosed as NASH, and 43 patients (32%) were SS. NASH patients were significantly older, predominantly female, hypertensive, more likely to have DM, had lower levels of hemoglobin (Hb), platelet count, albumin, cholinesterase and QUICKI, and had higher levels of AST, ALT, IRI, hyaluronic acid, type IV collagen 7S and HOMA-IR. Patients with NASH had lower levels of DHEA-S (108.8 ± 96.1 μg/dL) than those with SS (170.4 ± 129.2 μg/dL, $P = 0.003$). The AUC for DHEA in separating patients with and without NASH was 0.678 (Fig. 1a). The sensitivity of a DHEA-S-value of 99 μg/dL or less for the presence of NASH was 62.2% (56/90) and specificity was 67.4% (29/43).

Correlation between DHEA-S and other clinical variables in NAFLD patients

Levels of DHEA-S were positively correlated with Hb, platelet, ALT, cholinesterase, albumin and triglyceride, and negatively correlated with age, AST, AST/ALT ratio, ALP, HDL-C, hyaluronic acid and type IV collagen 7S. They had no associations with markers of insulin resistance such as HOMA-IR and QUICKI (Table 2). Serum DHEA-S levels were not different between patients with HOMA-IR of more than 2.5 ($n = 73$, 125.6 ± 116.0 μg/dL) and with HOMA-IR of less than 2.5 ($n = 57$, 134.4 ± 107.9 μg/dL, $P = 0.660$). Similarly, serum DHEA-S levels were not different between patients with QUICKI of more than 0.3 ($n = 102$, 123.7 ± 114.4 μg/dL) and with QUICKI of less than 0.3 ($n = 26$, 114.8 ± 108.2 μg/dL, $P = 0.448$).

Comparison between participants with simple steatosis, and mild and advanced NASH

Patients with NAFLD were divided into three groups, including SS, mild NASH (NASH with fibrosis stage 0–2) and advanced NASH (NASH with fibrosis stage 3–4). Female sex was more prevalent in patients with advanced NASH than in those with SS and mild NASH. Participants in the SS group were younger than participants with mild and advanced NASH. The prevalence of obesity and lifestyle-related diseases did not differ among three groups. Platelet count decreased in accordance with the incremental fibrosis of NAFLD. The AST/ALT ratio, fibrosis markers (hyaluronic acid, type IV collagen 7S) and insulin resistance were elevated in the advanced stage of NAFLD. Participants with advanced NASH had significantly lower levels of DHEA-S compared with participants with SS, and tended to have low